Cellular Microbiology (2010) **12**(6), 740–753
doi:10.1111/j.1462-5822.2010.01430.x
First published online 12 February 2010

Cryptococcus neoformans responds to mannitol by increasing capsule size *in vitro* and *in vivo*

Allan Jefferson Guimarães,[1,2†] Susana Frases,[1–3†] Radamés J. B. Cordero,[1,2] Leonardo Nimrichter,[4] Arturo Casadevall[1,2] and Joshua D. Nosanchuk[1,2*]
Departments of [1]Medicine (Division of Infectious Diseases) and [2]Microbiology and Immunology, Albert Einstein College of Medicine of Yeshiva University, Bronx, NY, USA.
[3]Laboratório de Biotecnologia (LABIO), Instituto Nacional de Metrologia, Normalização e Qualidade Industrial (INMETRO), Rio de Janeiro, Brazil.
[4]Laboratório de Estudos integrados em Bioquímica Microbiana, Instituto de Microbiologia Professor Paulo de Góes, Universidade Federal do Rio de Janeiro, Rio de Janeiro, Brazil.

Summary

The polysaccharide capsule of the fungus *Cryptococcus neoformans* is its main virulence factor. In this study, we determined the effects of mannitol and glucose on the capsule and exopolysaccharide production. Growth in mannitol significantly increased capsular volume compared with cultivation in glucose. However, cells grown in glucose concentrations higher than 62.5 mM produced more exopolysaccharide than cells grown in mannitol. The fibre lengths and glycosyl composition of capsular polysaccharide from yeast grown in mannitol was structurally different from that of yeast grown in glucose. Furthermore, mannitol treatment of mice infected intratracheally with *C. neoformans* resulted in fungal cells with significantly larger capsules and the mice had reduced fungal dissemination to the brain. Our results demonstrate the capacity of carbohydrate source and concentration to modify the expression of a major virulence factor of *C. neoformans.* These findings may impact the clinical management of cryptococcosis.

Received 18 September, 2009; revised 25 November, 2009; accepted 20 December, 2009. *For correspondence. E-mail nosanchu@aecom.yu.edu; Tel. (+1) 718 430 2993; Fax (+1) 718 430 8968.
†A.J.G. and S.F. contributed equally to this work.
The data in this paper are from a thesis to be submitted by Allan J. Guimarães in partial fulfillment of the requirements for the degree of Doctor of Philosophy in the Sue Golding Graduate Division of Medical Science, Albert Einstein College of Medicine, Yeshiva University, Bronx, NY, USA.

Introduction

Cryptococcosis is an opportunistic infection caused by the encapsulated yeast *Cryptococcus neoformans* (Cn). Cn has a worldwide distribution (Muller, 1994; Jain *et al.*, 2005) and is a major fungal pathogen in immunocompromized hosts, especially in individuals with HIV infection (Chayakulkeeree and Perfect, 2006; Park *et al.*, 2009). The fungus expresses a variety of well-defined and characterized virulence factors, including a polysaccharide (PS) capsule, a cell wall-associated laccase and released phospholipases (Kozel, 1995; Hamilton and Goodley, 1996; Buchanan and Murphy, 1998; Perfect *et al.*, 1998; Blackstock *et al.*, 1999; Mcclelland *et al.*, 2005). The capsule is Cn's most prominent virulence determinant, and acapsular strains are not able to cause disease in immunocompetent hosts (Fromtling *et al.*, 1982; Cross and Bancroft, 1995; Chang *et al.*, 1997). Furthermore, secreted Cn PS interferes with host responses to infection (Vecchiarelli, 2000).

The cryptococcal capsule is composed of two major PSs, glucuronoxylomannan (GXM) and galactoxylomannan (GalXM) (Doering, 2000; Mcfadden *et al.*, 2007; Frases *et al.*, 2008; Villena *et al.*, 2008; Yoneda and Doering, 2008). GXM comprises approximately 90% of the capsule and is formed by a linear (1→3)-α-d-mannopyranan main chain bearing β-d-xylopyranosyl (Xyl) in β(1→2) or β(1→4) linkages (Cherniak *et al.*, 1998a), (1→2)β-d-glucopyranosyluronic acid (GlcA) attached to every third mannose, on average, and 6-*O*-acetyl substituents (Kozel *et al.*, 1988; Cherniak *et al.*, 1998a, Reese and Doering, 2003; Mcfadden *et al.*, 2006a,b; Nimrichter *et al.*, 2007; Frases *et al.*, 2008). GalXM is an α(1→6)-galactan containing β(1, 3) oligosaccharyl substitutions at alternate residues of galactose. The oligosaccharide constituents of GalXM are trisaccharide motifs composed of α(1→3)-mannosyl dimers in α(1, 4) linkages to galactosyl units. Each of the trisaccharide components may be substituted with β(1→2)- or β(1→3)-xylosyl residues. In contrast to typical PS production, GXM appears to be synthesized in the cytoplasm and then transported to the cell surface by mechanisms involved in vesicular secretion (Yoneda and Doering, 2006; Rodrigues *et al.*, 2007). Regarding the capsular structure, O acetylation and/or xylosylation are important for binding of anti-GXM MAbs,

complement activation and GXM tissue (Janbon *et al*., 2001; Kozel *et al*., 2003).

Capsular PS thickness is regulated by environmental conditions, and strains with different phenotypes can be biased towards specific organs (Rivera *et al*., 1998; Zaragoza *et al*., 2003; Garcia-hermoso *et al*., 2004; Zaragoza and Casadevall, 2004). PS synthesis is especially increased by low ferric iron or high CO_2 concentrations, and the two effects are additive (Vartivarian *et al*., 1993; Zaragoza and Casadevall, 2004). Because of its relevance for Cn survival in different conditions capsular synthesis and assembly has been studied in details. Interestingly, recent physical studies have shown significant differences between capsular PS and exopolysaccharide, suggesting that these two fractions represent distinct biosynthetic products (Frases *et al*., 2008). Capsular growth can also be affected by different carbon sources (Onishi and Suzuki, 1968; Golubev and Manukian, 1979; Granger *et al*., 1985). Capsular production increases on media with lower amounts of glucose (Okabayashi *et al*., 2005); however, higher levels of exopolysaccharide occur in culture supernatants from high glucose media (Cleare and Casadevall, 1999). Additionally, mammalian serum or diluted Sabouraud broth efficiently induced capsule growth (Zaragoza and Casadevall, 2004).

Cryptococcus neoformans is known to produce D-mannitol *in vitro* (Onishi and Suzuki, 1968). Glucose concentration of 20% (w/v) induces mannitol production, consisting of 28% molar yield based upon glucose used (Onishi and Suzuki, 1968). Mannitol is also generated when fructose and mannose are used as carbon sources (Onishi and Suzuki, 1968). D-mannitol is also produced during cryptococcosis (Wong *et al*., 1990). In fact, concentrations of D-mannitol in cerebrospinal fluid (CSF) from rabbits infected with Cn correlated with CSF GXM content and the severity of infection. In humans, mannitol has been detected in 19 of 21 CSF samples evaluated (ranging from 1.5 to 26.2 mg l^{-1}; 0.8 μM to 0.14 mM, respectively), but there was no quantitative correlation between the mannitol concentration and the cryptococcal antigen titre (Megson *et al*., 1996).

D-mannitol is known to scavenge free radicals, reducing the ability of CSF phagocytes to kill Cn yeasts. Niehaus and Flynn (1994) showed that the ability of Cn to catabolize mannitol was constitutively expressed. However, it is not known whether D-mannitol regulates Cn virulence factors or if the carbohydrate impacts pathogenesis (Megson *et al*., 1996). In our current work, we sought to evaluate the effect of mannitol on the capsular regulation of Cn. We applied diverse methods, including dynamic light scattering to analyse the dimensions of PS molecules, light microscopy and immunofluorescence, to determine capsule size and GXM properties. We also determined the concentration of GXM in different capsules formed under the different growth conditions and evaluated the importance of capsule thickness induced by mannitol *in vivo*.

Results

Carbon sources regulate capsular size in a dose-dependent fashion

The growth rate of Cn was similar in all the conditions tested (data not shown). To evaluate the impact of carbon source on capsular growth, Cn yeasts were cultivated in minimal medium containing mannitol or glucose and then stained with Indian ink to assess the capsule volume. Mannitol significantly increased capsule growth compared with glucose over a concentration range of 7.8–500 mM ($P < 0.001$) (Fig. 1A). Maximum capsular volume was observed in media with 125 mM of mannitol ($18094 \pm 501.4\ \mu m^3$) (Fig. 1B), followed by media containing 62.5 and 31.25 mM mannitol. Capsular volumes were significantly smaller in the presence of glucose, reaching their maximum size at 62.5 and 15.63 mM ($3633 \pm 226\ \mu m^3$ and $4387 \pm 306\ \mu m^3$, respectively) (Fig. 1B), followed by concentrations of 250 and 125 mM. In addition, when compared with mannitol, a larger cell body size was observed in cells cultivated in glucose concentrations higher than 62.5 mM (Fig. 1B). Except for the condition containing mannitol at 125 mM, in which a clearer zone surrounding the cell body was observed, the large capsules in cells cultivated in mannitol were more diffuse, with a higher penetration of India ink particles into regions surrounding the cell body.

Capsular PS and exopolysaccharide production are regulated by the type of carbon source

Changes in the antigenic properties of capsular PSs may occur *in vivo* (Rivera *et al*., 1998; Guerrero *et al*., 2006). In order to establish the relative amount of reactive epitopes present on the capsule and exopolysaccharide, we performed ELISA assays with monoclonal antibodies to GXM (18B7) (Casadevall *et al*., 1998). The reactivity of mAb 18B7 to capsular and secreted PSs obtained from yeasts cultivated with different carbon sources was evaluated by ELISA. The greatest capsule volume and highest concentration of PS measured by ELISA was observed with media containing 125 mM of mannitol ($P < 0.001$, Fig. 1C). For glucose, maximal capsular epitope production was observed at 250 mM (43.4 vs. 30.7 mg ml^{-1} of GXM for mannitol, $P < 0.001$; Fig. 1C). At carbon source concentrations ≥ 250 mM, PS from cells grown in glucose displayed more binding to epitopes recognizable by mAb 18B7 than cells cultured in mannitol ($P < 0.001$). This effect was reversed for concentrations between 125 and 31.25 mM, where mannitol induced a larger capsule

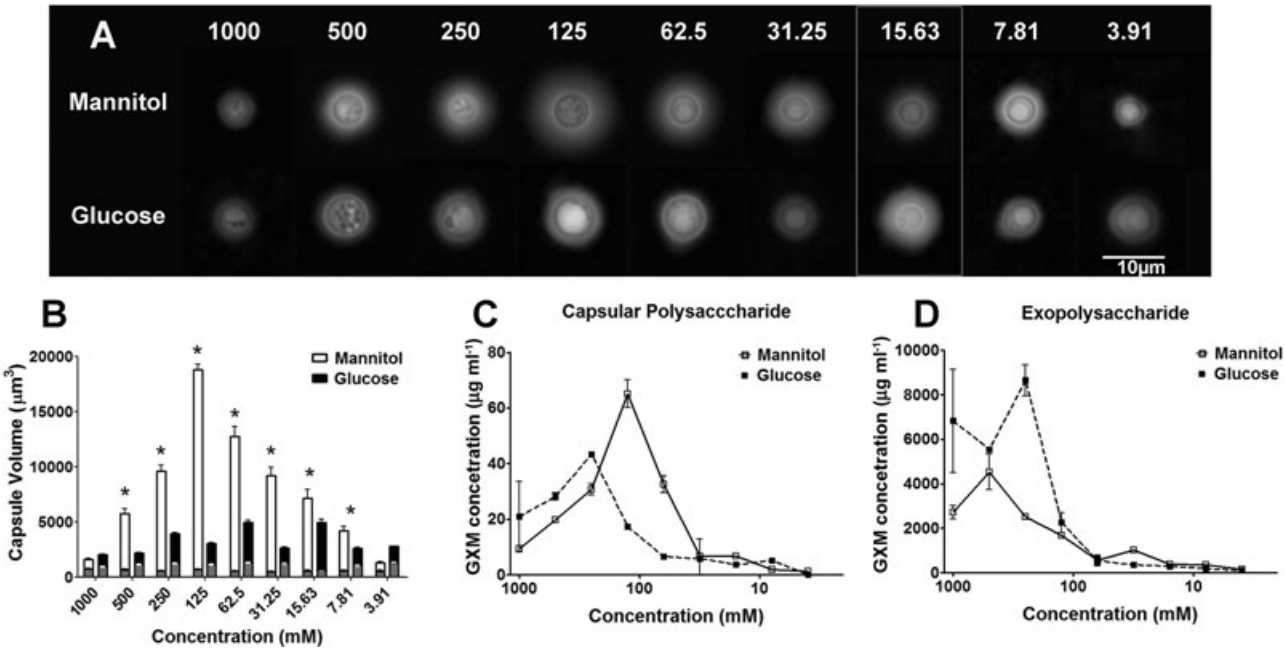

Fig. 1. Effect of mannitol and glucose on *C. neoformans* capsule and polysaccharide production. *C. neoformans* yeasts were grown in different concentrations of mannitol and glucose, and their effects on the capsule were evaluated.
A. India ink staining of *C. neoformans* yeasts. Scale bar = 10 µm.
B. Capsular volumes were determined by measuring total cell volume (cell body and capsule) and subtracting the cell body volume. White bars show the capsular volumes for cells grown in mannitol. Black solid bars show capsular volumes for cells grown in glucose. Grey bars show the cell body volume for each condition evaluated. Graphs show the average of at least 100 Cn cells evaluated. *$P < 0.001$.
C. The quantity of capsular polysaccharide epitopes was determined using a capture ELISA. Graphs show the average of three different experiments.
D. The concentration of exopolysaccharide epitopes in supernatants was determined by ELISA showing a different dynamic than the capsular polysaccharide epitope production. Graphs show the average of three different experiments.

than glucose. When lower carbohydrate concentrations were used, no statistical difference in either capsule size or reactivity was observed. The highest concentrations of exopolysaccharide from Cn grown in glucose were observed at 250 mM (8665 mg ml^{-1}) and from cultures with 500 mM of mannitol (4530 mg ml^{-1}). Additionally, yeasts grown in glucose concentrations higher than 125 mM ($P < 0.001$) produced more exopolysaccharide than cells incubated in mannitol. For concentrations lower than 125 mM, no statistical difference was observed between the groups ($P > 0.05$; Fig. 1D). Differences in kinetics of capsular and exopolysaccharide production further suggest that there is a differential regulation in the production of these two pools of PSs or they are generated by two different biosynthetic pathways.

Carbon source alters capsular thickness and surface distribution of antigen epitopes recognized by mAb 18B7

Chitin staining with Uvitex 3BSA and direct immunofluorescence with antibodies to GXM permitted relative measurements of capsular thickness and epitope distribution for mAb 18B7 (Fig. 2A). In all the conditions tested, mAb 18B7 bound to Cn cells in an annular fashion (Torres *et al.*, 2005). However, substantial differences in capsule thickness and epitope distribution were apparent between the different conditions tested. Cells grown in media containing ≥ 125 mM mannitol displayed a thicker capsule, with diffuse capsular binding and fluorescence (Fig. 2A). Cells grown in ≥ 250 mM glucose showed a smaller and well-defined outer ring, and less fluorescence distributed towards the cell body. At 125 mM glucose, the capsule was smaller and binding was more diffused. Smaller capsules were present at concentrations ≤ 62.5 mM of both sugars and no substantial differences were observed. Additionally, cells cultivated in either sugar at these concentrations had a smaller, but very bright and dense compartment between the cell wall and the capsule.

When the number of epitopes recognized by 18B7 was compared with the volume of the capsule calculated from the cellular radius and cell body length, we observed that the distribution of epitopes on the cell surface was constant for cells grown in all mannitol concentrations, despite the differences in capsule size, and a Pearson correlation was observed ($P = 0.0017$, Pearson $r = 0.88$; Fig. 2B). Lower mannitol concentrations induced a higher ratio of epitopes/capsule volume. Additionally, yeasts grown in glucose had

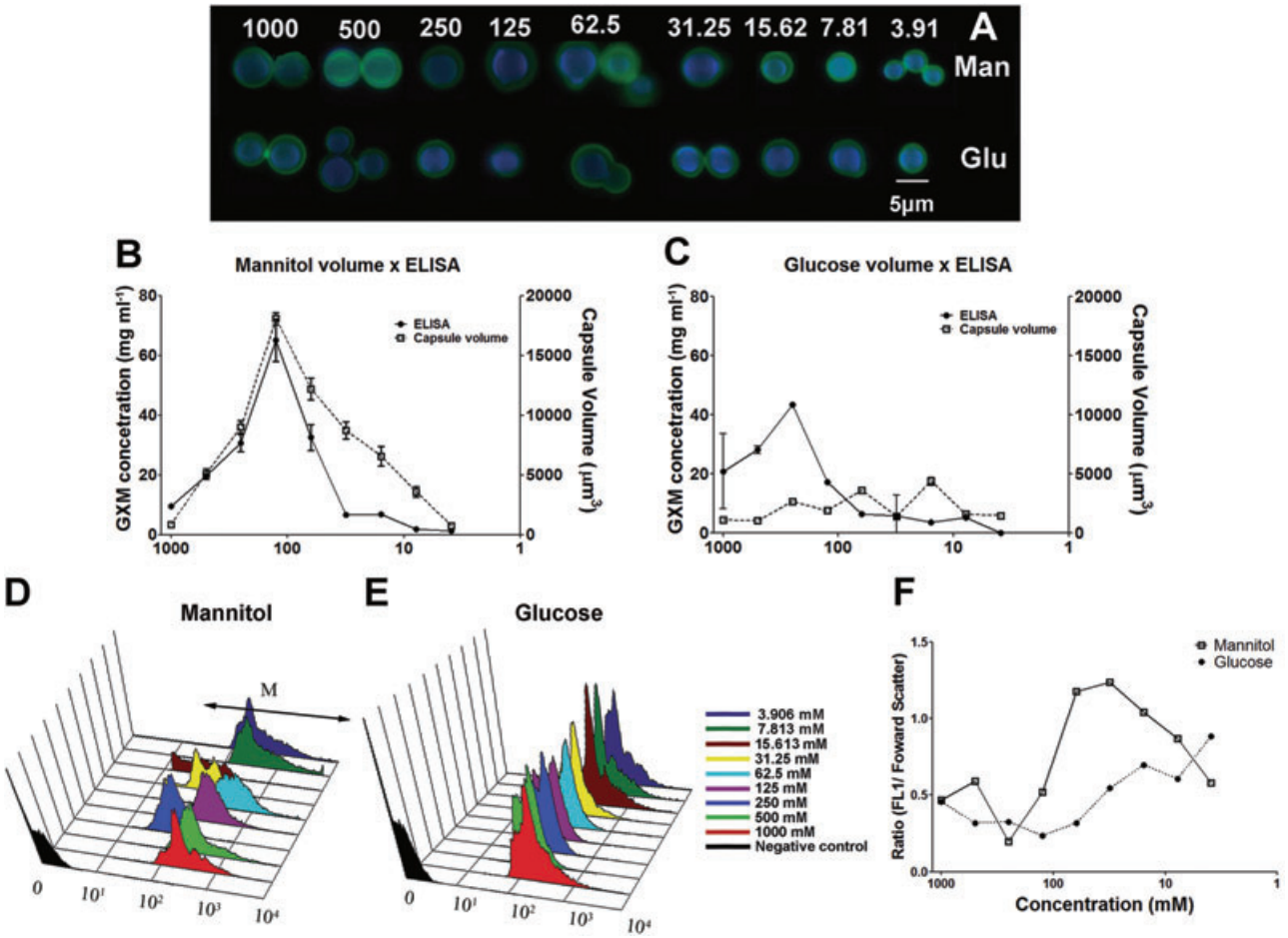

Fig. 2. Distribution of epitopes on the capsule of *C. neoformans* cells grown in different concentrations of mannitol and glucose.
A. Direct immunofluorescence at similar exposure times show differences in binding and brightness intensity, suggesting a different density of epitopes in each growth condition considered. Scale bar = 10 µm.
B. Epitope concentration in the capsule obtained by capture ELISA correlated positively with capsular volume from mannitol calculated by India ink staining; however, in concentrations lower than 62.5 mM, epitope concentration was higher.
C. A similar effect was observed for cells grown on glucose.
D. and E. FACS analysis showing the fluorescence intensity of cells after binding of FITC-labelled 18B7 mAb for cells grown in (D) mannitol and (E) glucose.
F. Fluorescence intensity (FL1-H) normalized by cell diameter (FSC-H) values show a higher density of epitopes for both carbon sources when cells were grown in concentrations lower that 62.5 mM.

a much lower epitope/capsule volume ratio, which was nearly constant under the different concentrations used (Fig. 2C). However, no correlation was observed between capsule size and GXM concentration in glucose medium ($P = 0.68$, Pearson $r = -0.62$).

When intensity of fluorescence was compared by fluorescence-activated cell sorting (FACS) in order to confirm the amount of capsular epitopes after labelling the capsule with FITC-conjugated mAb 18B7, yeasts grown in either mannitol or glucose showed a decrease in fluorescence intensity relative to cells grown in lower concentrations of carbon sources (Fig. 2D and E, respectively, $P < 0.05$). When lower concentrations were used, despite the decrease in the fluorescence, the cell diameter also decreased considerably, as estimated from FSC-H values. Normalization of fluorescence intensity (FL1-H) by cell diameter inferred from FSC-H values resulted in a slight increase in the ratio, suggesting a higher density of epitopes for both carbon sources when cells were grown in concentrations lower that 62.5 mM (Fig. 2F, $P < 0.05$). These results correlated with the immunofluorescence and ELISAs/cell volume ratio studies. Additionally, we also observed that Cn cells tended to aggregate at carbon concentrations < 62.5 mM, giving a higher FL1-H signal of each particle detected.

Carbon source influences capsule composition

As the capsules of Cn cells displayed differences in volume and epitope distribution, we sought to determine

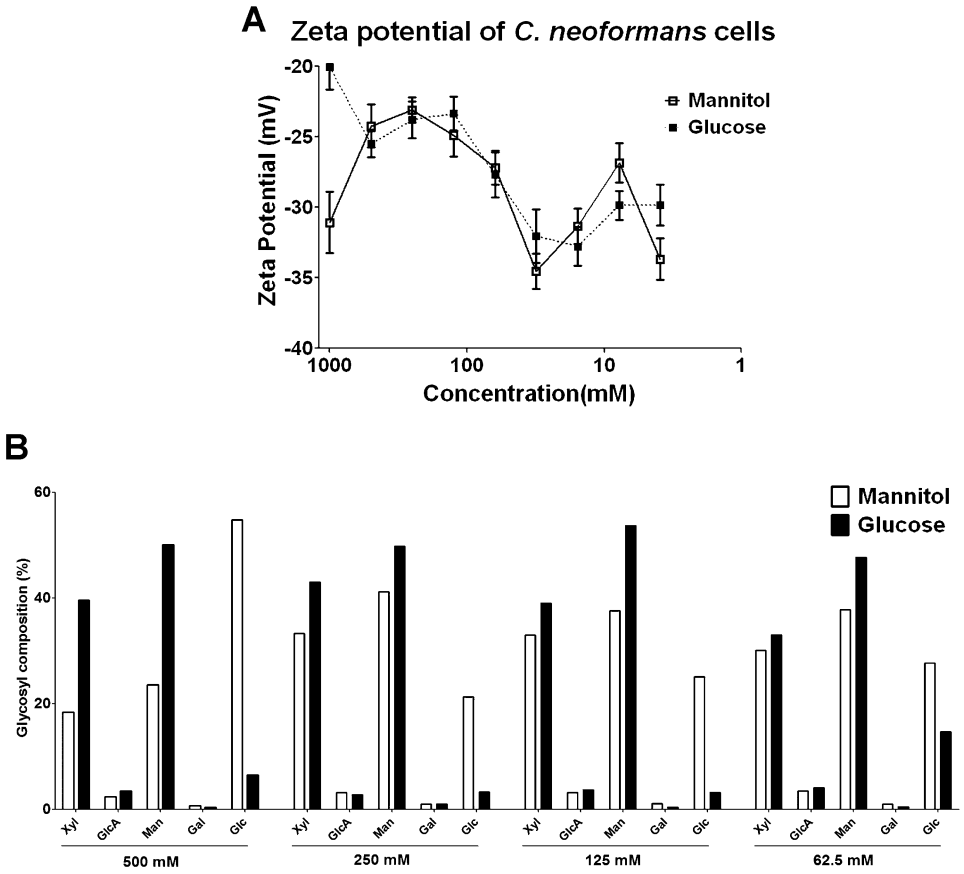

Fig. 3. Determinations of cell charge and glycosyl composition of capsular polysaccharide show different capsular contents.
A. Zeta potential of cells grown in different concentrations of mannitol and glucose show a similar cell charge for cells grown in both sugars.
B. Glycosyl composition of the capsular polysaccharide of cells grown in different concentrations of mannitol and glucose indicate a different stoichiometry in calpsular composition. Xyl, xylose; GlcA, glucuronic acid; Man, mannose; Gal, galactose; Glc, glucose.

whether different carbon sources could alter the capsular chemical composition. For instance, metabolic changes could alter the expression of biosyntethic enzymes or production of the PSs precursors, resulting in a different capsular structure and composition. Zeta potential measurements indicate the charges surrounding a cell surface and our measurements demonstrated that the carbon source impacted cell charge (Fig. 3A). At concentrations between 500 and 3.9 mM, cell charge measurements were similar for cells grown with either sugar. Cell charge increased in magnitude at lower concentrations in a similar manner for both sugars. In contrast, cells grown in media containing 1000 mM mannitol manifested increased negative charge whereas 1000 mM glucose induced a significant reduction in the negative charge. Notably, the trend in both curves was very similar to the curve of 18B7 binding detected on the cell capsule under each condition (mannitol, $P = 0.07$, Pearson $r = 0.64$ and glucose, $P = 0.03$, Pearson $r = 0.71$) (Fig. 1C). This suggests that cell charge is directly proportional to the amount of epitopes on the capsule of Cn yeast cells for either carbon source used.

In order to characterize the sugar composition of the Cn capsule, we measured the ratios of each component monosaccharides. We observed that PS from cells grown in glucose contained more mannose residues compared with cells grown in mannitol ($P < 0.001$). However, glucose was shown to be more frequent in capsules of Cn yeasts grown in mannitol ($P < 0.001$). These effects were less pronounced when the carbon source concentrations were below 62.5 mM. The average molar ratios of cells grown in either glucose or mannitol are shown in Fig. 3B. Except for the cells grown in 500 mM of mannitol, where glucose was the major component, the general order of molar composition was mannose, followed by xylose and glucose for both carbon sources. Slight increases in the amount of glucuronic acid residues in PS from cells grown in either sugar accounted for the decreasing of the Zeta potential as described previously (Nosanchuk and Casadevall, 1997; Frases *et al.*, 2008).

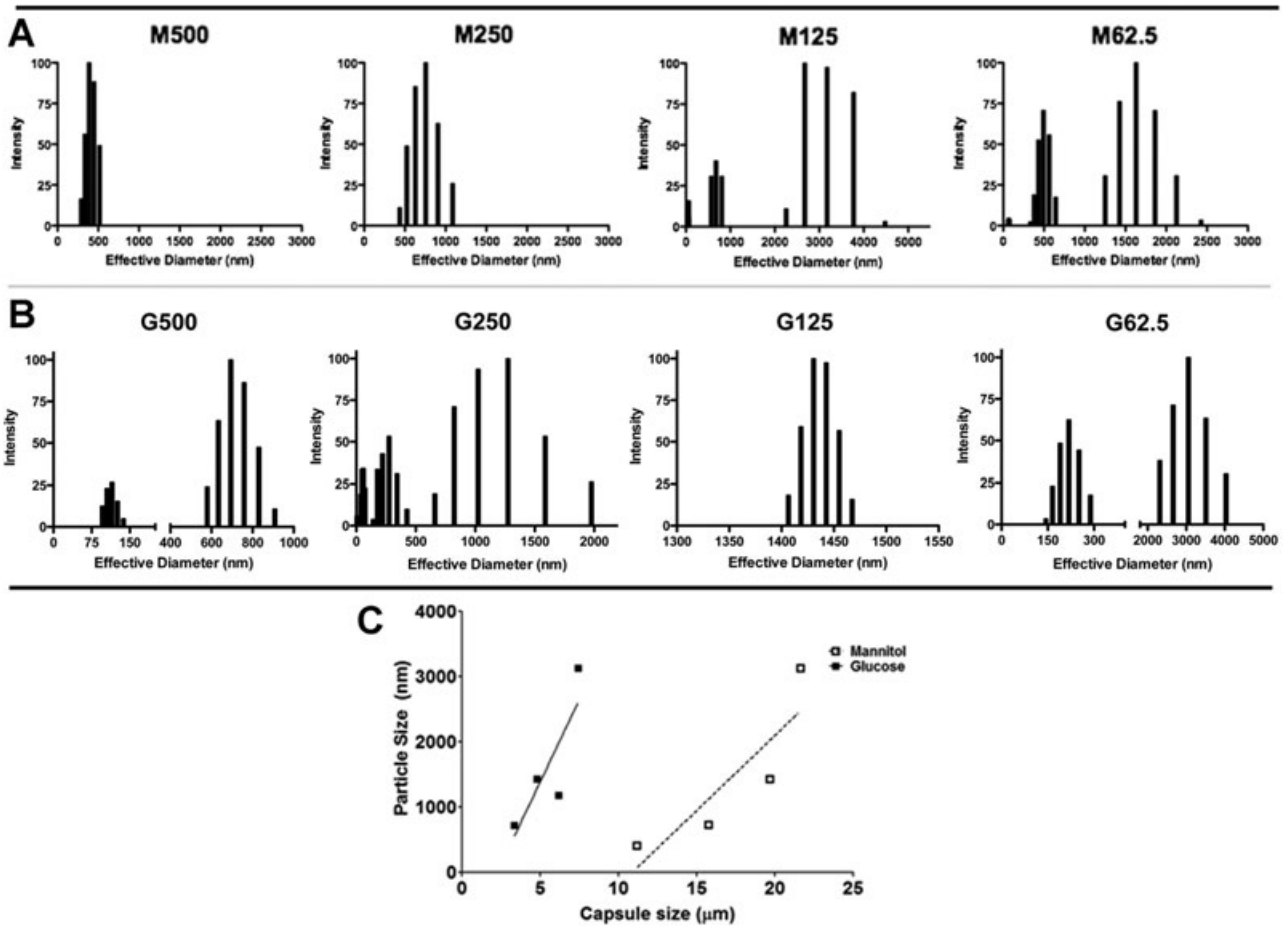

Fig. 4. Dynamic light scattering (DLS) analysis and multimodal size distribution of capsular PS from strain H99 grown in different concentrations of (A) mannitol [M] and (B) glucose [G]. The *x*-axis represents the distribution of fibres diameter measured in nanometres; *y*-axis corresponds to the values of percentage intensity weighted sizes obtained from the NNLS algorithm.
C. Correlation between capsule size measured by India ink negative stain and average of capsular PS and multimodal size distribution analysis of capsular PS by DLS.

Carbon source affects the formation of capsular PS fibres

To analyse the structure of the capsular PS at the molecular level, we used dynamic light scattering to provide some information about size distribution and frequency of the fibres forming the PS (Fig. 4). When mannitol was used as carbon source, the largest PS fibres were observed at 125 mM, followed by 62.5, 250 and 500 mM, correlating with the light microscopy data for capsule size. A linear correlation was obtained using the average of capsule diameter calculated by India ink measurements versus the diameter of PS fragments ($R^2 = 0.77$; $P < 0.05$; Fig. 4C). Interestingly, when the mannitol concentration was diminished, two or more dominant populations were observed in the capsule of Cn yeasts. Cells cultivated in glucose had a different pattern of PS fibre production. The largest fibres were observed when yeasts were grown in 62.5 mM of glucose, followed by 250, 500 and 125 mM. These findings corresponds with the largest capsule size for this group as measured by light microscopy, and an additional correlation was obtained between capsule diameter and diameter of PS fragments ($R^2 = 0.71$; $P < 0.05$, Fig. 4C).

In vivo *supplementation with carbohydrates impacts the pathogenesis of cryptococcosis*

We tested whether the *in vivo* administration of either glucose or mannitol would alter the pathogenesis of cryptococcosis. In our model, mice given PBS, glucose or mannitol had similar pulmonary colony-forming units (cfu) (Fig. 5A, 4.26×10^7, 7.17×10^7 and 8.90×10^7 yeasts g^{-1} respectively). However, brain cfu in mice treated with mannitol was 2-logs lower than control (Fig. 5B, 1.23×10^3 vs. 1.89×10^5 yeast g^{-1}; $P < 0.05$) or glucose-treated animals (5.20×10^3 yeasts g^{-1}; $P < 0.05$).

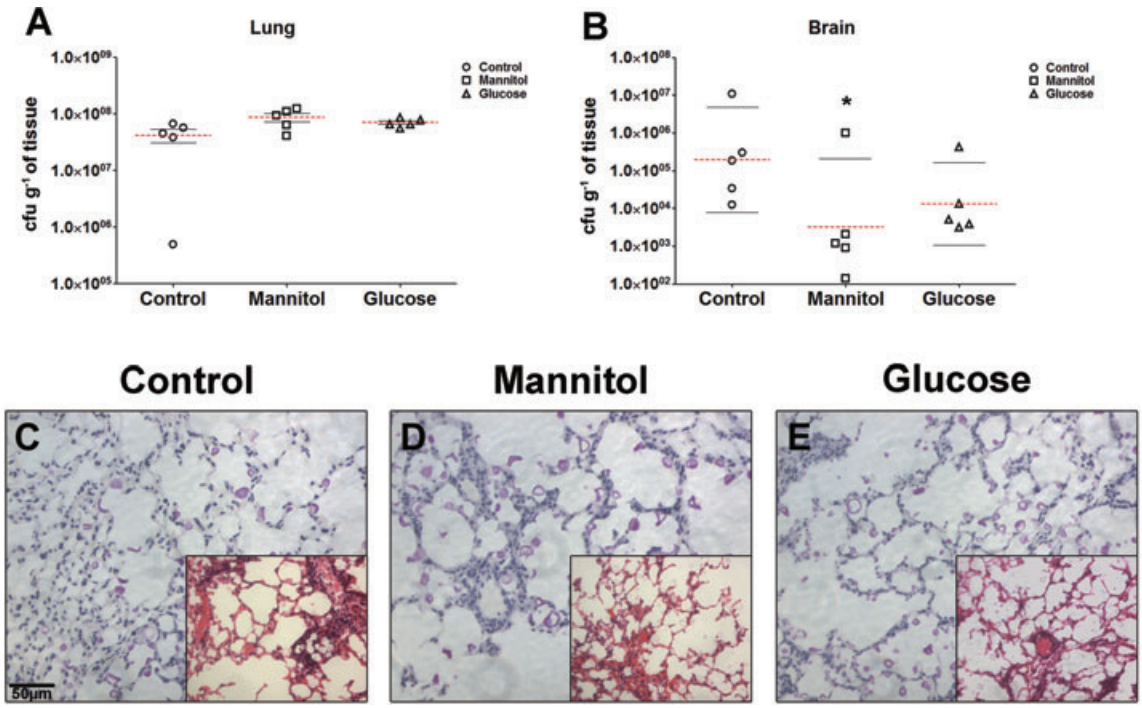

Fig. 5. *In vivo* role of mannitol and glucose infusions on the outcome of cryptococcosis after intratracheal *C. neoformans* infection.
A. Lung cfu determinations after 5 days of infection show similar values for mannitol- and glucose-treated and control mice.
B. Brain cfu were lower in mannitol-treated mice (*$P < 0.05$). The results shown represent one of three independent experiments, each of which produced consistent data.
C.–E. Mucicarmine staining of lungs from (C) control (D) mannitol and (E) glucose show yeast capsular polysaccharide stained in pink. Insets on each respective figure display tissue inflammation by H&E. Scale bar = 50 μm.

Histological analysis

Histological examination revealed differences in cellular responses in the lungs of mannitol- or glucose-treated and control animals. The lungs of the infected animals exhibited foci of inflammatory reaction, granulomatous inflammation composed of macrophages and epithelioid cells, surrounded by perivascular lymphocytes and neutrophils (Fig. 5C–E). A large collection of extracellular Cn yeast cells could also be observed in the alveolar, perivascular spaces and parenchyma, as well as some intracellular yeast trapped in the interior of numerous granulomas. Notably, a greater numbers of extracellular yeasts were present in the lung parenchyma of mannitol- ($45.9 \pm 15.6\%$, $P < 0.05$) and glucose- ($25.5 \pm 4.7\%$, $P < 0.05$) treated animals compared with controls ($11.7 \pm 7.1\%$).

Cn cells show differential capsule/cell body ratio in vivo *depending on carbon sources*

Organ homogenates of infected mice were visualized by direct immunofluorescence with antibody to GXM to identify Cn yeast cells *in vivo*. Cn from lung homogenates displayed thicker capsules compared with yeast cells identified in suspensions from brain (Fig. 6A and B, respectively). Although there were fewer yeast cells, there were no differences in cell or capsule size in the fungi isolated from the brain after glucose or mannitol treatment. However, when mannitol was administered, a substantial increase was observed in capsule of yeasts in the lung tissues, despite the smaller cell body diameter, which then increased the capsule volume/cell body volume ratio (8.62; $P < 0.05$; Fig. 6C and E). Glucose and control groups had similar values for capsule volume/cell body volume ratio of yeast isolated from lungs (3.92 and 4.50, respectively; Fig. 6B and D). This also corroborates the previous result showing the difference in capsule volume as observed *in vitro*.

GXM production is regulated by presence of mannitol in vivo

The amount of soluble GXM was measured in different tissues and serum of mice challenged with Cn in the presence or absence of mannitol and glucose. GXM levels in lung and serum positively correlated with host fungal burden. There was a trend to a higher GXM levels in serum of mannitol-treated mice (0.48 ± 0.37 μg ml^{-1}) relative to the glucose (0.046 ± 0.041 μg ml^{-1}) and control animals (0.070 ± 0.037 μg ml^{-1}), but this differ-

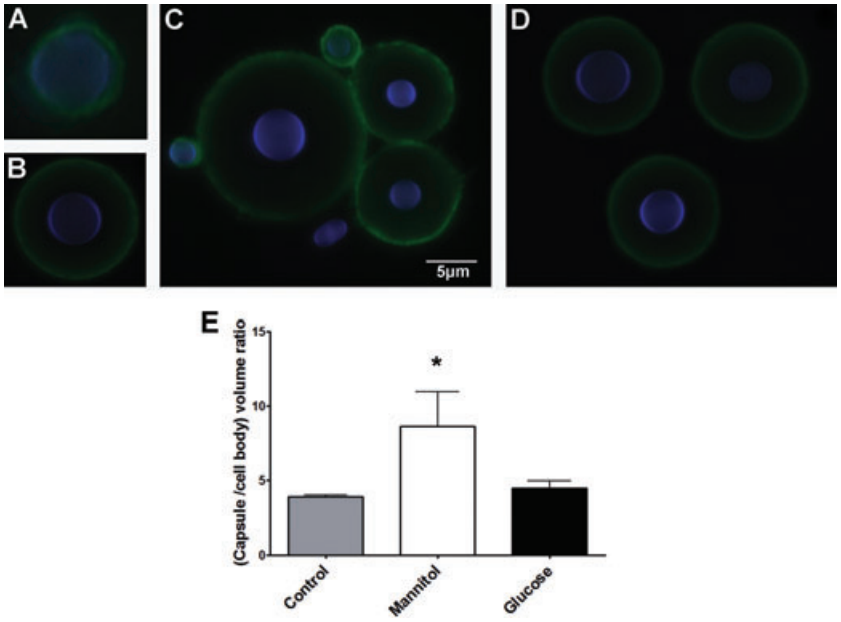

Fig. 6. Direct immunofluorescence with *C. neoformans* cells isolated from lung and brains of mice 5 days after infection.
A. and B. Yeasts isolated from brain showed a much smaller capsule when compared with cells isolated from lung (B) of control mice.
C. Cells isolated from lungs of mice treated with mannitol had thicker capsules compared with controls.
D. Cells isolated from lungs of animals treated with glucose did not show any difference compared with controls. Scale bar = 10 μm.
E. Ratios of capsule/cell body volumes suggest a much more effective mechanism of mannitol cells *in vivo* regarding capsular production (*$P < 0.001$).

ence was not statistically significant (data not shown). We also evaluated the distribution of GXM in lung and brains of infected animals. In the lungs, the highest GXM values were obtained in organ homogenates of animals treated with mannitol (74.73 ± 17.7 μg ml^{-1}, $P = 0.03$) when compared with glucose (49.99 ± 3.5 μg ml^{-1}) and control groups (26.90 ± 11.4 μg ml^{-1}) (Fig. 7A); however, glucose and control groups were statistically similar In contrast, the GXM levels in brains of infected control animals were significantly higher than in mice from the mannitol and glucose groups (0.43 ± 0.40 vs. 0.017 ± 0.012 and 0.019 ± 0.005 μg ml^{-1}, respectively; $P < 0.05$, Fig. 7B), and the GXM levels correlated with the brain cfu.

Discussion

This study began when we attempted to use mannitol to osmotically stabilize extracellular vesicle formation (Sethi and Maeda, 1983; van Rooijen and van Nieuwmegen, 1984; van Rooijen *et al*., 2003) in cryptococcal cultures and improve the yield of vesicles and serendipitously observed that supplementation of media with mannitol had a tremendous effect on capsule size. The physiological significance of mannitol secretion by Cn in its native milieu and *in vivo* is still unclear. Cn produces D-mannitol *in vitro* and *in vivo*. D-mannitol has been identified in cerebral and pulmonary cryptococcomas (Himmelreich *et al*., 2003; Dzendrowskyj *et al*., 2005), and D-mannitol has been characterized as a quantitative marker for experimental cryptococcal meningitis (Wong *et al*., 1990). However, concentrations of mannitol in the microenvironment of cerebral and pulmonary cryptococcomas have

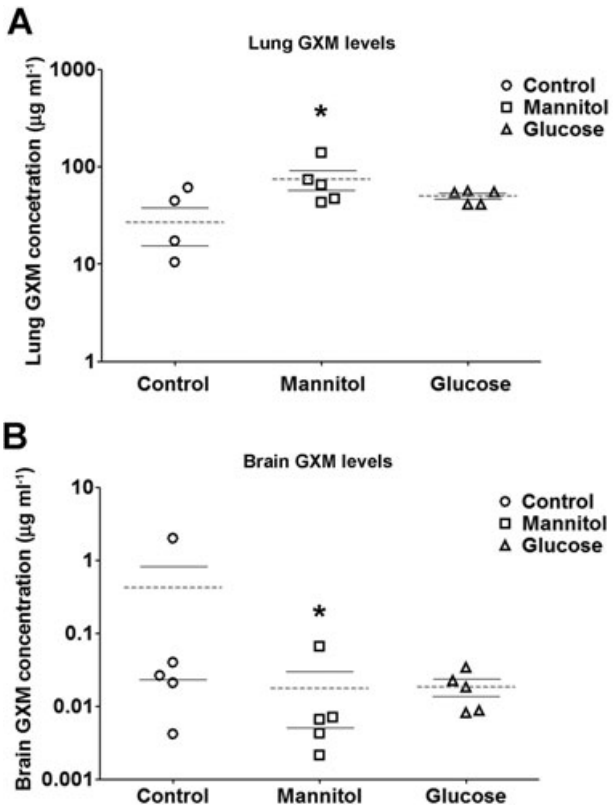

Fig. 7. Inhibition ELISA quantification of GXM levels in the lungs (A) and brains (B) of mice treated with or without glucose or mannitol. The levels correlated with tissue cfu determinations (*$P < 0.05$). Mean values and standard deviations from five different mice are plotted.

not been determined, and might be much higher than the maximum value reported for CSF and serum (50 mM) (Megson *et al*., 1996; Garcia-morales *et al*., 2004). Yeast polyol metabolism through mannitol has been considered as a potential biochemical pathway for virulence (Perfect *et al*., 1998), as a non-mannitol-producing mutant strain of Cn was about two orders of magnitude less virulent than its parental strain (Wong *et al*., 1990). Despite the well-characterized D-mannitol secretion and its correlation to the degree of virulence, the effects of D-mannitol on capsule production of Cn have not been explored. Cn yeasts can use mannitol as the sole carbon source and incorporate this sugar intact to the capsule, as the carbon chain of mannitol is not altered by the yeast (Cherniak *et al*., 1998a).

To evaluate these effects, we investigated the modulation of capsular growth *in vitro* and the outcome of infected mice in the presence of mannitol and glucose. The *in vitro* experiments demonstrated that mannitol induced a thicker capsule of Cn cells when added to cryptococcal cultures in the range within 500 and 7.81 mM. The highest difference was observed when concentrations of 125 mM of both sugars were used, resulting in mannitol grown cells with capsule volumes 10 times larger than glucose grown cells. When we evaluated the amount of PSs using an ELISA, mannitol grown cells had greater reactivity in the capsule, about four times higher when compared with glucose grown cells. However, higher amounts of epitopes recognized by this antibody were observed only in mannitol concentrations of 125 and 62.5 mM. Yeasts grown in glucose were able to produce and secrete more PS than yeasts grown in mannitol at concentrations higher than 125 mM. These results, along with the capsular volume, show a different regulation in terms of capsular and exopolysaccharide production dependent on concentration and carbon sources used. Furthermore, as we observed that higher exopolysaccharide productions did not always correlate with higher capsular PS production, capsular and exopolysaccharide could yet constitute different biosynthetic products from different PS pathway production.

Different physical chemical properties impact binding of antibody to GXM. The reactivity of these PSs with the 18B7 antibody was additionally evaluated by FACS; and these data were correlated with cell size. A better reactivity was observed for cells with smaller capsules, when the fluorescence intensity was normalized by cell size, suggesting that structural differences in the capsular PSs could result in antigenic differences (Charlier *et al*., 2005; Frases *et al*., 2008).

To characterize possible capsular structural differences, we measured Zeta potential and analysed the glycosyl composition of capsular PSs extracted from the yeasts. Although the concentrations of sugars altered cell charge, values were similar between the carbon sources used when a similar concentration was considered, except at 1000 mM where mannitol increased the negative cell charge and glucose reduced the negative charge. In all the samples tested, mole percentage of mannose was higher than the mole percentage of xylose. GXM from H99 strain of Cn in chemically defined liquid medium is expected to display the PS motif M2 (mannose$_3$-glucuronic acid-xylose$_2$) (Cherniak *et al*., 1991; 1998b). However, we observed that the concentration and carbon source impacted the sugar concentration and thus, as the molar ratio of the PSs differed, other reported motifs could be produced (for example, M5). Further characterization of PS fractions obtained from these cells by light scattering demonstrated significant structural differences. For instance, cells grown in 125 mM mannitol produced the largest PS fibres, which correlated with the largest India ink exclusion zone. With the other concentrations evaluated, capsular fibres of glucose grown yeasts were always larger than mannitol grown yeasts. However, as the capsule thickness for cells grown in mannitol was much larger, the shorter PS fibres must associate with either different branching formations or aggregate – via cationic bridges – to form a thicker capsule. Furthermore, as the fluorescence intensity was similar for cells with a larger capsule compared with cells with a smaller capsule, epitope accessibility and exposure is impacted by the carbohydrate substrate and concentration.

It is unclear whether the effects of mannitol on capsule induction are due to alterations in metabolic pressure, with incorporation of the intact sugar into the capsule, or if this simple carbohydrate works as a quorum sensing molecule, as it is produced by the fungus during its growth (Molloy, 2006). *In vivo*, the role of mannitol as a metabolic product remains unclear. However, we created a mouse model by administering therapeutic doses (based on dosages used clinically) and compared with glucose. Mannitol treatment resulted in a reduction in the dissemination of Cn to the brain. These results are consistent with the findings that Cn mutants that cannot downregulate their capsule have impaired phagocytosis and extrapulmonary dissemination and (Casadevall and Perfect, 1998; Shea *et al*., 2006). Animals receiving glucose also had a reduction in dissemination, although their capsules in the lung were not significantly larger than Cn isolated from controls. However, in this situation a different explanation may be operative. Systemic glucose administration could have induced a transient diabetic state in mice that increased susceptibility to infection, given that hyperglycaemia causes macrophage dysfunction and caused inhibition of tumour necrosis factor production (Satomi *et al*., 1985; Kawakami *et al*., 1996; Liu *et al*., 1999), which in turn could have reduced dissemination in macrophages.

Tissue GXM levels correlated with the cfu determinations and the capsular size of the yeast in the respective tissues. Although GXM can be cleared from serum over several days (Lendvai *et al.*, 1998), deposition in organs and the presence of GXM in serum has diverse adverse effects on immune cell function (Retini *et al.*, 1996), including downregulation of T-cell responses (Vecchiarelli, 2007), inhibition of neutrophil chemotaxis (Dong and Murphy, 1996; Monari *et al.*, 2002) and impared macrophage killing (Monari *et al.*, 2003).

Mannitol is clinically utilized as a hyperosmolar agent for the treatment of intracranial hypertension (ICP) and as a diuretic and anti-hypertensive (Sakowitz *et al.*, 2007). This polyol prevents visual loss and other neurological sequelae because of high ICP (Bhardwaj, 2007), by setting up an osmotic gradient across the blood–brain barrier (osmotherapy) reducing CSF pressure. D-mannitol is also present in the CSF of patients with cryptococcal meningitis, and this produced sugar competes with intravenous D-mannitol osmotherapy because of its inability to cross the blood brain barrier, increasing the CSF pressure and leading to oedema formation. Hence, secretion of D-mannitol by Cn may contribute to cerebral oedema. Secretion may also increase the microbe's tolerance of heat and osmotic stresses and interfere with phagocytic killing by scavenging reactive oxygen species, resulting in an enhancement in Cn pathogenicity (Chaturvedi *et al.*, 1996a,b).

High mannitol concentrations in CSF has been also positively correlated with high titres of cryptococcal antigen (Wong *et al.*, 1990) and high intracranial pressure (Megson *et al.*, 1996; Liappis *et al.*, 2008). Pathogenesis of raised ICP tends to occur in patients with prolonged disease, and this prognosis is strongly correlated with high cryptococcal antigen titres (Saag *et al.*, 2000). The possible mechanism of increased CSF osmolality is related to the production of high-molecular-weight cryptococcal PS, induced by the accumulation of mannitol, and also the presence of a large burden of yeasts plugging the arachnoid villi, reducing the outflow gradient of CSF. Mannitol that has crossed the blood–brain barrier, and the mannitol produced by the fungus may draw fluid into the central nervous system, aggravating then the vasogenic oedema. Other serious effects are permanent neurological sequelae such as reduced visual acuity, blindness, papilloedema and deafness. Our results have clinical implications as mannitol has been administered during severe cases of cryptococcosis for the treatment of increased ICP, but this medical intervention has not been effective (Saag *et al.*, 2000). This study showing the regulatory role of mannitol on capsule biosynthesis and Cn virulence further suggests that mannitol therapy is relatively contraindicated for cryptococcosis.

Experimental procedures

Fungal cultures

Cryptococcus neoformans ATCC H99 was grown in chemically defined medium composed of $MgSO_4$ (10 mM), KH_2PO_4 (29.4 mM), glycine (13 mM) and thiamine-HCl (3 μM), pH 5.5 and supplemented with 1000, 500, 250, 125, 62.5, 31.25, 15.6, 7.8 and 3.9 mM of either glucose or mannitol as carbon sources. For all experiments, Cn were cultivated for 2 days at 30°C with rotary shaking. Growth in different conditions was evaluated in cultures starting with 10^6 yeasts ml^{-1}, and growth curves were obtained photometrically (Bioscreen C, Growth Curves USA, NJ, USA). Cell density after 48 h of growth was confirmed using a haematocytometer.

Light microcopy and India ink staining

Samples were prepared from each condition by dilutions in PBS according to haemocytometer counts. An aliquot of each Cn culture was mixed with a drop of India ink (BD Biosciences, NJ, USA) and examined using an Axiovert 200 M inverted microscope (Carl Zeiss Micro Imaging, NY). Images were collected with a 40× lens and photographed with an AxiocamMR camera controlled by AxioVision 4.4 software. Capsule size was measured in ImageJ 1.39g software (National Institutes of Health, NIH, Bethesda, MD) as the distance between capsule border and the cell wall, corresponding to the India ink exclusion zone. At least 100 Cn yeasts were measured for each growth condition.

GXM ELISA

An inhibition ELISA was developed for the detection of capsular and exopolysaccharides from cultures on different growth conditions. Initially, a 96-well polystyrene plate (NUNC) (reaction plate) was coated with 50 μl of a 10 mg ml^{-1} purified GXM diluted in PBS and incubated overnight at 4°C. Reaction plates were washed three times with TBS-T (10 mM Tris-HCl, 150 mM NaCl, 1 mM NaN_3, 0.1% Tween 20, pH 7.4) and blocked with 200 μl of blocking solution [2% (w/v) bovine serum albumin in TBS-T] for 1 h at 37°C. A second polystyrene 96-round-well microtitre plate (Nunc A/S, Kamstrup, Denmark) (inhibition plate) was also blocked for 1 h at 37°C with the same blocking buffer. After blocking the ELISA plates were washed with PBS. A standard GXM curve with concentrations ranging from 10 to 0.0565 mg ml^{-1} (obtained by 1:3 serial dilutions) was constructed, and 50 μl of each concentration was added to the inhibition plate in duplicate. To measure the capsular PS, 10^5 washed Cn yeasts from each condition were added to the wells in duplicate. To measure the extracellular PS, the supernatant samples were diluted 1:10 and 50 μl were added to the wells in duplicate. Cn cells and extracellular PS samples were diluted across the plate. Fifty microlitres of a 4 mg ml^{-1} solution of the mAb to GXM 18B7 (Casadevall *et al.*, 1998) was added to all wells on the inhibition plate and then incubated for 2 h at 37°C. The content of the inhibition plate was then transferred to the respective wells in the reaction plate. The excess of antibody to GXM was allowed to interact with GXM adsorbed to the reactive plate for 1 h at 37°C. Plate wells were then washed three times and coated with 50 μl of a 1:1500 dilution of alkaline phosphatase-conjugated goat anti-mouse immunoglobulin G1 (IgG1) (Southern Biotechnology)

in blocking buffer and incubated for 1 h at 37°C. Plates were then washed and incubated with 50 μl well^{-1} of 1 mg ml^{-1} p-nitrophenyl phosphate diluted in substrate buffer (1 mM $MgCl_26H_2O$, 0.05 M Na_2CO_3, pH 9.8) for 30 min at room temperature. Absorbance was measured at 405 nm on an ELISA plate reader (μQuant Microplate Spectrophotometer, BioTek Instruments, Winooski, VT, USA). All determinations were done in triplicate, and the average of three different experiments was considered.

Immunofluorescence with antibody to capsule

Aliquots from each growth condition containing 5×10^6 Cn yeasts were transferred to microcentrifuge tubes. Cells were quickly spun down to remove excess of liquid and suspended in 100 μl of a 100 mg ml^{-1} solution of 18B7 mAb in blocking solution. Tubes were incubated in an orbital shaker for 1 h at 37°C. Cells were washed three times with TBS-T by centrifugation. The pellets were then suspended in 100 μl of a 1:100 dilution in blocking solution of a FITC-conjugated goat anti-mouse IgG1 (Southern Biotechnology). Tubes were incubated for 1 h at 37°C and then washed with TBS-T. Pellets were suspended in mounting solution (Biomeda Corp, Foster City, CA) and the suspension applied to a microscopy slide. Cells were examined with an Olympus AX70 fluorescence microscope using a 495 nm filter, with a magnificence of 40×.

Fluorescence-activated cell sorting

Cryptococcus neoformans (10^6) were transferred to a microcentrifuge tube and incubated for 1 h at 37°C with 10 mg ml^{-1} of a FITC-conjugated mAb 18B7 diluted in PBS. Yeasts were washed, and the fluorescence intensity of cells analysed in a FACScan Flow Cytometer (BD Biosciences, Franklin Lakes, NJ). A forward side scatter (FSC) versus fluorescence (FL1) graphs was plotted.

Zeta potential measurements

A total of 10^5 yeast cells were washed three times with MilliQ water and suspended in pure distilled lipopolysaccharide-free water. Zeta potential (ζ), particle mobility and shift frequency were analysed comparing the different zeta potentials on cells from growth in different carbon sources. These measurements were calculated in a Zeta potential analyser (ZetaPlus, Brookhaven Instruments Corp., Holtsville, NY). ζ is a measurement of charge (in mV) defined as the potential gradient that develops across the interface between a boundary liquid in contact with a solid and the mobile diffuse layer in the body of the liquid. It is derived from the equation $\zeta = (4\pi\eta m)/D$, where D is the dielectric constant of the medium, η is the viscosity, and m is the electrophoretic mobility of the particle.

Light scattering and particle sizes of capsular PSs

Capsular PS was isolated as described (Frases *et al.*, 2009). Yeast cells were washed three times in water, suspended in five-cell pellet volumes of dimethylsulfoxide and incubated at room temperature for 30 min. This procedure was done twice, and the fractions were pooled. Cells were centrifuged for 1100 *g* for 10 min and supernatant collected. This fraction was then dialysed against distilled water for 12 h, with water changes for at least six times. These capsular PS preparations were analysed by QELS in a 90Plus/BI-MAS Multi Angle Particle Sizing analyser (Brookhaven Instruments) and the effective diameter and polydispersity measured. Effective diameter is considered the diameter of the imaginary coaxial cylinder that intersects the surface of the thread. Polydispersity is a measure of the distribution of molecular mass in a complex mixture of polymers and indicates the distribution of individual molecular masses.

Glycosyl composition of extracted capsular PSs

Extracted capsular PS preparations were lyophilized, and PS fractions were dissolved in methanol/1M HCl and incubated at 80°C for 18 h. Methanolysed samples were then per-*O*-trimethylsilylated by treatment with Tri-Sil (Pierce) for 30 min at 80°C. The per-*O*-TMS derivatives were analysed by gas chromatography coupled to mass spectrometry (GC-MS). The derivatized structures were first separated on an HP 5890 gas chromatograph using a Supelco DB-1 fused silica capillary column (30 m × 0.25 mm ID). Peaks detected by GC were fragmented in a 5970 MSD mass spectrometer, interfaced to the gas chromatograph. Carbohydrate standards included arabinose, rhamnose, fucose, xylose, glucuronic acid, galacturonic acid, mannose, galactose, glucose, mannitol, dulcitol and sorbitol. The percentage of each element was measured as a function of thermal conductivity. Elemental ratios were calculated by dividing the percentage of each element measured in the sample by its respective atomic weight. The values reported are from two independent analysis using different sample batches.

In vivo *model*

Animal procedures were approved by the Institute for Animal Studies of the Albert Einstein College of Medicine. Four to six week BALB/c mice (National Cancer Institute) received 100 μl of intraperitoneal injections of a 20% (w/v) solution of glucose or mannitol every 8 h for 12 consecutive days. Glucose or mannitol was administered intraperitoneally in a dose corresponding to the *in vivo* administration of mannitol used for the management of increased intracranial pressure (approximately 1.5 g kg^{-1}) (Rudehill *et al.*, 1993; Silva *et al.*, 2009; Singhi and Tiwari, 2009). Control mice received PBS. At day 7 of treatment, mice were infected intratracheally with 10^7 yeast cells. At day 12, the mice were killed, brains and lungs were immediately removed, and sections of each organ were fixed in a formalin solution and stained with H&E for histology. Slides were observed with an Olympus AX70 microscope using a bright field, with a magnificence of 20×.

The remaining excised brain and lung tissues were weighed and then homogenized using 70 μm cell strainers (BD Biosciences, NJ, USA) in PBS buffer. Organ homogenates were serially diluted and plated in duplicates on Sabouraud Dextrose Agar plates (Difco Laboratories). After 2 days of incubation at 30°C, the number of colonies was enumerated. Capsule dimensions in organ homogenates was also measured by mixing an aliquot of the lung or brain homogenates with India ink. Coverslips were applied and the slides and the cells observed as described. Additionally, immunofluorescence with the mAb 18B7

using brain and lung homogenates was performed. Briefly, 100 μl of brain or lung homogenate was placed on a slide microcentrifuge tube and immunofluorescence done as described above. Twenty microlitres of 1% Uvitex 3BSA-PBS (Ciba-Geigy, Greensboro, NC) were added to the samples and incubated for 10 min. Uvitex 3BSA binds chitin in the yeast cell wall and was used to delineate the cell wall. Samples were visualized by immunofluorescence microscopy as described.

Finally, an inhibition ELISA to detect GXM in organ supernatants was performed as above, with GXM standard curve ranging from 2 μg ml^{-1} to 0.98 ng ml^{-1}, with 0.25 μg ml^{-1} of mAb 18B7.

Statistical analyses

All statistical analyses were performed using GraphPad Prism version 5.00 for Windows (GraphPad Software, San Diego, CA, USA). A one-way ANOVA using a Kruskall-Wallis non-parametrical test was used to statistically compare the differences among groups, and an individual comparison between groups was done by Bonferoni post test. A 95% confidence interval was considered in all experiments.

Acknowledgements

A.J.G. and L.N. were supported in part by an Interhemispheric Research Training Grant in Infectious Diseases, Fogarty International Center (NIH D43-TW007129). A.J.G and J.D.N. are supported in part by NIH AI52733 and the Center for AIDS Research at the Albert Einstein College of Medicine and Montefiore Medical Center (NIH AI-51519). L.N. is supported by grants from Conselho Nacional de Desenvolvimento Tecnológico (CNPq, Brazil) and Fundação Carlos Chagas Filho de Amparo à Pesquisa do Estado do Rio de Janeiro (FAPERJ, Brazil). R.J.B.C was supported by the Training Program in Cellular and Molecular Biology and Genetics, T32 GM007491.

References

Bhardwaj, A. (2007) Osmotherapy in neurocritical care. *Curr Neurol Neurosci Rep* **7:** 513–521.

Blackstock, R., Buchanan, K.L., Cherniak, R., Mitchell, T.G., Wong, B., Bartiss, A., *et al.* (1999) Pathogenesis of *Cryptococcus neoformans* is associated with quantitative differences in multiple virulence factors. *Mycopathologia* **147:** 1–11.

Buchanan, K.L., and Murphy, J.W. (1998) What makes *Cryptococcus neoformans* a pathogen? *Emerg Infect Dis* **4:** 71–83.

Casadevall, A., and Perfect, J. (1998) *Cryptococcus Neoformans*. Washington, DC: ASM Press.

Casadevall, A., Cleare, W., Feldmesser, M., Glatman-Freedman, A., Goldman, D.L., Kozel, T.R., *et al.* (1998) Characterization of a murine monoclonal antibody to *Cryptococcus neoformans* polysaccharide that is a candidate for human therapeutic studies. *Antimicrob Agents Chemother* **42:** 1437–1446.

Chang, Y.C., Cherniak, R., Kozel, T.R., Granger, D.L., Morris, L.C., Weinhold, L.C., and Kwon-Chung, K.J. (1997) Structure and biological activities of acapsular *Cryptococcus neoformans* 602 complemented with the CAP64 gene. *Infect Immun* **65:** 1584–1592.

Charlier, C., Chretien, F., Baudrimont, M., Mordelet, E., Lortholary, O., and Dromer, F. (2005) Capsule structure changes associated with *Cryptococcus neoformans* crossing of the blood-brain barrier. *Am J Pathol* **166:** 421–432.

Chaturvedi, V., Flynn, T., Niehaus, W.G., and Wong, B. (1996a) Stress tolerance and pathogenic potential of a mannitol mutant of *Cryptococcus neoformans*. *Microbiology* **142** (Part 4)**:** 937–943.

Chaturvedi, V., Wong, B., and Newman, S.L. (1996b) Oxidative killing of *Cryptococcus neoformans* by human neutrophils. Evidence that fungal mannitol protects by scavenging reactive oxygen intermediates. *J Immunol* **156:** 3836–3840.

Chayakulkeeree, M., and Perfect, J.R. (2006) Cryptococcosis. *Infect Dis Clin North Am* **20:** 507–544, v–vi.

Cherniak, R., Morris, L.C., Anderson, B.C., and Meyer, S.A. (1991) Facilitated isolation, purification, and analysis of glucuronoxylomannan of *Cryptococcus neoformans*. *Infect Immun* **59:** 59–64.

Cherniak, R., O'Neill, E.B., and Sheng, S. (1998a) Assimilation of xylose, mannose, and mannitol for synthesis of glucuronoxylomannan of *Cryptococcus neoformans* determined by 13C nuclear magnetic resonance spectroscopy. *Infect Immun* **66:** 2996–2998.

Cherniak, R., Valafar, H., Morris, L.C., and Valafar, F. (1998b) *Cryptococcus neoformans* chemotyping by quantitative analysis of 1H nuclear magnetic resonance spectra of glucuronoxylomannans with a computer-simulated artificial neural network. *Clin Diagn Lab Immunol* **5:** 146–159.

Cleare, W., and Casadevall, A. (1999) Scanning electron microscopy of encapsulated and non-encapsulated *Cryptococcus neoformans* and the effect of glucose on capsular polysaccharide release. *Med Mycol* **37:** 235–243.

Cross, C.E., and Bancroft, G.J. (1995) Ingestion of acapsular *Cryptococcus neoformans* occurs via mannose and beta-glucan receptors, resulting in cytokine production and increased phagocytosis of the encapsulated form. *Infect Immun* **63:** 2604–2611.

Doering, T.L. (2000) How does *Cryptococcus* get its coat? *Trends Microbiol* **8:** 547–553.

Dong, Z.M., and Murphy, J.W. (1996) Cryptococcal polysaccharides induce l-selectin shedding and tumor necrosis factor receptor loss from the surface of human neutrophils. *J Clin Invest* **97:** 689–698.

Dzendrowskyj, T.E., Dolenko, B., Sorrell, T.C., Somorjai, R.L., Malik, R., Mountford, C.E., and Himmelreich, U. (2005) Diagnosis of cerebral cryptococcoma using a computerized analysis of 1H NMR spectra in an animal model. *Diagn Microbiol Infect Dis* **52:** 101–105.

Frases, S., Nimrichter, L., Viana, N.B., Nakouzi, A., and Casadevall, A. (2008) *Cryptococcus neoformans* capsular polysaccharide and exopolysaccharide fractions manifest physical, chemical, and antigenic differences. *Eukaryot Cell* **7:** 319–327.

Frases, S., Pontes, B., Nimrichter, L., Viana, N.B., Rodrigues, M.L., and Casadevall, A. (2009) Capsule of *Cryptococcus neoformans* grows by enlargement of polysaccharide molecules. *Proc Natl Acad Sci USA* **106:** 1228–1233.

Fromtling, R.A., Shadomy, H.J., and Jacobson, E.S. (1982) Decreased virulence in stable, acapsular mutants of *Cryptococcus neoformans*. *Mycopathologia* **79:** 23–29.

Garcia-Hermoso, D., Dromer, F., and Janbon, G. (2004) *Cryptococcus neoformans* capsule structure evolution *in vitro* and during murine infection. *Infect Immun* **72:** 3359–3365.

Garcia-Morales, E.J., Cariappa, R., Parvin, C.A., Scott, M.G., and Diringer, M.N. (2004) Osmole gap in neurologic-neurosurgical intensive care unit: Its normal value, calculation, and relationship with mannitol serum concentrations. *Crit Care Med* **32:** 986–991.

Golubev, V.I., and Manukian, A.R. (1979) [Capsule formation in saprophytic yeasts]. *Mikrobiologiia* **48:** 314–318.

Granger, D.L., Perfect, J.R., and Durack, D.T. (1985) Virulence of *Cryptococcus neoformans*. Regulation of capsule synthesis by carbon dioxide. *J Clin Invest* **76:** 508–516.

Guerrero, A., Jain, N., Goldman, D.L., and Fries, B.C. (2006) Phenotypic switching in *Cryptococcus neoformans*. *Microbiology* **152:** 3–9.

Hamilton, A.J., and Goodley, J. (1996) Virulence factors of *Cryptococcus neoformans*. *Curr Top Med Mycol* **7:** 19–42.

Himmelreich, U., Allen, C., Dowd, S., Malik, R., Shehan, B.P., Mountford, C., and Sorrell, T.C. (2003) Identification of metabolites of importance in the pathogenesis of pulmonary cryptococcoma using nuclear magnetic resonance spectroscopy. *Microbes Infect* **5:** 285–290.

Jain, N., Wickes, B.L., Keller, S.M., Fu, J., Casadevall, A., Jain, P., *et al.* (2005) Molecular epidemiology of clinical *Cryptococcus neoformans* strains from India. *J Clin Microbiol* **43:** 5733–5742.

Janbon, G., Himmelreich, U., Moyrand, F., Improvisi, L., and Dromer, F. (2001) Cas1p is a membrane protein necessary for the O-acetylation of the *Cryptococcus neoformans* capsular polysaccharide. *Mol Microbiol* **42:** 453–467.

Kawakami, K., Qifeng, X., Tohyama, M., Qureshi, M.H., and Saito, A. (1996) Contribution of tumour necrosis factor-alpha (TNF-alpha) in host defence mechanism against *Cryptococcus neoformans*. *Clin Exp Immunol* **106:** 468–474.

Kozel, T.R. (1995) Virulence factors of *Cryptococcus neoformans*. *Trends Microbiol* **3:** 295–299.

Kozel, T.R., Pfrommer, G.S., Guerlain, A.S., Highison, B.A., and Highison, G.J. (1988) Role of the capsule in phagocytosis of *Cryptococcus neoformans*. *Rev Infect Dis* **10** (Suppl. 2)**:** S436–S439.

Kozel, T.R., Levitz, S.M., Dromer, F., Gates, M.A., Thorkildson, P., and Janbon, G. (2003) Antigenic and biological characteristics of mutant strains of *Cryptococcus neoformans* lacking capsular O acetylation or xylosyl side chains. *Infect Immun* **71:** 2868–2875.

Lendvai, N., Casadevall, A., Liang, Z., Goldman, D.L., Mukherjee, J., and Zuckier, L (1998) Effect of immune mechanisms on the pharmacokinetics and organ distribution of cryptococcal polysaccharide. *J Infect Dis* **177:** 1647–1659.

Liappis, A.P., Kan, V.L., Richman, N.C., Yoon, B., Wong, B., and Simon, G.L. (2008) Mannitol and inflammatory markers in the cerebral spinal fluid of HIV-infected patients with cryptococcal meningitis. *Eur J Clin Microbiol Infect Dis* **27:** 477–479.

Liu, B.F., Miyata, S., Kojima, H., Uriuhara, A., Kusunoki, H., Suzuki, K., and Kasuga, M. (1999) Low phagocytic activity of resident peritoneal macrophages in diabetic mice: relevance to the formation of advanced glycation end products. *Diabetes* **48:** 2074–2082.

McClelland, E.E., Perrine, W.T., Potts, W.K., and Casadevall, A. (2005) Relationship of virulence factor expression to evolved virulence in mouse-passaged *Cryptococcus neoformans* lines. *Infect Immun* **73:** 7047–7050.

McFadden, D., Zaragoza, O., and Casadevall, A. (2006a) The capsular dynamics of *Cryptococcus neoformans*. *Trends Microbiol* **14:** 497–505.

McFadden, D.C., De Jesus, M., and Casadevall, A. (2006b) The physical properties of the capsular polysaccharides from *Cryptococcus neoformans* suggest features for capsule construction. *J Biol Chem* **281:** 1868–1875.

McFadden, D.C., Fries, B.C., Wang, F., and Casadevall, A. (2007) Capsule structural heterogeneity and antigenic variation in *Cryptococcus neoformans*. *Eukaryot Cell* **6:** 1464–1473.

Megson, G.M., Stevens, D.A., Hamilton, J.R., and Denning, D.W. (1996) D-mannitol in cerebrospinal fluid of patients with AIDS and cryptococcal meningitis. *J Clin Microbiol* **34:** 218–221.

Molloy, S. (2006) Quorum sensing: Fungal quorum sensing: in vino veritas? *Nature Reviews Microbiology* **4**.

Monari, C., Kozel, T.R., Bistoni, F., and Vecchiarelli, A. (2002) Modulation of C5aR expression on human neutrophils by encapsulated and acapsular *Cryptococcus neoformans*. *Infect Immun* **70:** 3363–3370.

Monari, C., Retini, C., Casadevall, A., Netski, D., Bistoni, F., Kozel, T.R., and Vecchiarelli, A. (2003) Differences in outcome of the interaction between *Cryptococcus neoformans* glucuronoxylomannan and human monocytes and neutrophils. *Eur J Immunol* **33:** 1041–1051.

Muller, J. (1994) [Pathogenesis, immunobiology and epidemiology of cryptococcosis]. *Mycoses* **37** (Suppl. 1)**:** 34–42.

Niehaus, W.G., and Flynn, T. (1994) Regulation of mannitol biosynthesis and degradation by *Cryptococcus neoformans*. *J Bacteriol* **176:** 651–655.

Nimrichter, L., Frases, S., Cinelli, L.P., Viana, N.B., Nakouzi, A., Travassos, L.R., *et al.* (2007) Self-aggregation of *Cryptococcus neoformans* capsular glucuronoxylomannan is dependent on divalent cations. *Eukaryot Cell* **6:** 1400–1410.

Nosanchuk, J.D., and Casadevall, A. (1997) Cellular charge of *Cryptococcus neoformans*: contributions from the capsular polysaccharide, melanin, and monoclonal antibody binding. *Infect Immun* **65:** 1836–1841.

Okabayashi, K., Kano, R., Watanabe, S., and Hasegawa, A. (2005) Expression of capsule-associated genes of *Cryptococcus neoformans*. *Mycopathologia* **160:** 1–7.

Onishi, H., and Suzuki, T. (1968) Production of d-mannitol and glycerol by yeasts. *Appl Microbiol* **16:** 1847–1852.

Park, B.J., Wannemuehler, K.A., Marston, B.J., Govender, N., Pappas, P.G., and Chiller, T.M. (2009) Estimation of the current global burden of cryptococcal meningitis among persons living with HIV/AIDS. *AIDS* **23:** 525–530.

Perfect, J.R., Wong, B., Chang, Y.C., Kwon-Chung, K.J., and Williamson, P.R. (1998) *Cryptococcus neoformans*: virulence and host defences. *Med Mycol* **36** (Suppl. 1)**:** 79–86.

Reese, A.J., and Doering, T.L. (2003) Cell wall alpha-1,3-glucan is required to anchor the *Cryptococcus neoformans* capsule. *Mol Microbiol* **50:** 1401–1409.

Retini, C., Vecchiarelli, A., Monari, C., Tascini, C., Bistoni, F., and Kozel, T.R. (1996) Capsular polysaccharide of *Cryptococcus neoformans* induces proinflammatory cytokine release by human neutrophils. *Infect Immun* **64:** 2897–2903.

Rivera, J., Feldmesser, M., Cammer, M., and Casadevall, A. (1998) Organ-dependent variation of capsule thickness in *Cryptococcus neoformans* during experimental murine infection. *Infect Immun* **66:** 5027–5030.

Rodrigues, M.L., Nimrichter, L., Oliveira, D.L., Frases, S., Miranda, K., Zaragoza, O., *et al.* (2007) Vesicular polysaccharide export in *Cryptococcus neoformans* is a eukaryotic solution to the problem of fungal trans-cell wall transport. *Eukaryot Cell* **6:** 48–59.

van Rooijen, N., and van Kesteren-Hendrikx, E. (2003) '*In vivo*' depletion of macrophages by liposome-mediated 'suicide'. *Methods Enzymol* **373:** 3–16.

van Rooijen, N., and van Nieuwmegen, R. (1984) Elimination of phagocytic cells in the spleen after intravenous injection of liposome-encapsulated dichloromethylene diphosphonate. An enzyme-histochemical study. *Cell Tissue Res* **238:** 355–358.

Rudehill, A., Gordon, E., Ohman, G., Lindqvist, C., and Andersson, P. (1993) Pharmacokinetics and effects of mannitol on hemodynamics, blood and cerebrospinal fluid electrolytes, and osmolality during intracranial surgery. *J Neurosurg Anesthesiol* **5:** 4–12.

Saag, M.S., Graybill, R.J., Larsen, R.A., Pappas, P.G., Perfect, J.R., Powderly, W.G., *et al.* (2000) Practice guidelines for the management of cryptococcal disease. Infectious Diseases Society of America. *Clin Infect Dis* **30:** 710–718.

Sakowitz, O.W., Stover, J.F., Sarrafzadeh, A.S., Unterberg, A.W., and Kiening, K.L. (2007) Effects of mannitol bolus administration on intracranial pressure, cerebral extracellular metabolites, and tissue oxygenation in severely head-injured patients. *J Trauma* **62:** 292–298.

Satomi, N., Sakurai, A., and Haranaka, K. (1985) Relationship of hypoglycemia to tumor necrosis factor production and antitumor activity: role of glucose, insulin, and macrophages. *J Natl Cancer Inst* **74:** 1255–1260.

Sethi, M., and Maeda, E. (1983) Studies on wheat protoplasts: a rapid and large-scale isolation method and cell wall regeneration in cultures. *Jpn J Crop Sci* **52:** 158–167.

Shea, J.M., Kechichian, T.B., Luberto, C., and Del Poeta, M. (2006) The cryptococcal enzyme inositol phosphosphingolipid-phospholipase C confers resistance to the antifungal effects of macrophages and promotes fungal dissemination to the central nervous system. *Infect Immun* **74:** 5977–5988.

Silva, J.C., de Melo Tavares de Lima, F., Valenca, M.M., and de Azevedo Filho, H.R. (2009) Hypertonic saline more efficacious than mannitol in lethal intracranial hypertension model. *Neurol Res* DOI: 10.1179/174313209X405119.

Singhi, S.C., and Tiwari, L. (2009) Management of intracranial hypertension. *Indian J Pediatr* **76:** 519–529.

Torres, M., May, R., Scharff, M.D., and Casadevall, A. (2005) Variable-region-identical antibodies differing in isotype demonstrate differences in fine specificity and idiotype. *J Immunol* **174:** 2132–2142.

Vartivarian, S.E., Anaissie, E.J., Cowart, R.E., Sprigg, H.A., Tingler, M.J., and Jacobson, E.S. (1993) Regulation of cryptococcal capsular polysaccharide by iron. *J Infect Dis* **167:** 186–190.

Vecchiarelli, A. (2000) Immunoregulation by capsular components of *Cryptococcus neoformans*. *Med Mycol* **38:** 407–417.

Vecchiarelli, A. (2007) Fungal capsular polysaccharide and T-cell suppression: the hidden nature of poor immunogenicity. *Crit Rev Immunol* **27:** 547–557.

Villena, S.N., Pinheiro, R.O., Pinheiro, C.S., Nunes, M.P., Takiya, C.M., DosReis, G.A., *et al.* (2008) Capsular polysaccharides galactoxylomannan and glucuronoxylomannan from *Cryptococcus neoformans* induce macrophage apoptosis mediated by Fas ligand. *Cell Microbiol* **10:** 1274–1285.

Wong, B., Perfect, J.R., Beggs, S., and Wright, K.A. (1990) Production of the hexitol d-mannitol by *Cryptococcus neoformans in vitro* and in rabbits with experimental meningitis. *Infect Immun* **58:** 1664–1670.

Yoneda, A., and Doering, T.L. (2006) A eukaryotic capsular polysaccharide is synthesized intracellularly and secreted via exocytosis. *Mol Biol Cell* **17:** 5131–5140.

Yoneda, A., and Doering, T.L. (2008) Regulation of *Cryptococcus neoformans* capsule size is mediated at the polymer level. *Eukaryot Cell* **7:** 546–549.

Zaragoza, O., and Casadevall, A. (2004) Experimental modulation of capsule size in *Cryptococcus neoformans*. *Biol Proced Online* **6:** 10–15.

Zaragoza, O., Fries, B.C., and Casadevall, A. (2003) Induction of capsule growth in *Cryptococcus neoformans* by mammalian serum and CO(2). *Infect Immun* **71:** 6155–6164.